



## Research article

Metabologenomics approach to the discovery of novel compounds from *Streptomyces* sp. GMR22 as anti-SARS-CoV-2 drugsYohana Nadia Melinda<sup>a</sup>, Jaka Widada<sup>b,\*</sup>, Tutik Dwi Wahyuningsih<sup>c</sup>, Rifki Febriansah<sup>d,e</sup>, Ema Damayanti<sup>a,f</sup>, Mustofa Mustofa<sup>d</sup><sup>a</sup> Study Program of Biotechnology, Graduate School of Universitas Gadjah Mada, Jl. Teknik Utara, Pogung, Mlati, Sleman, Yogyakarta 55281, Indonesia<sup>b</sup> Department of Agricultural Microbiology, Faculty of Agriculture, Universitas Gadjah Mada, Yogyakarta 55281, Indonesia<sup>c</sup> Department of Chemistry, Faculty of Natural Science and Mathematics, Universitas Gadjah Mada, Yogyakarta 55281, Indonesia<sup>d</sup> Department of Pharmacology and Therapy, Faculty of Medicine, Public Health, and Nursing, Universitas Gadjah Mada, Yogyakarta, Indonesia<sup>e</sup> Faculty of Medicine and Health Sciences, University of Muhammadiyah Yogyakarta, Indonesia<sup>f</sup> Research Division for Natural Product Technology, National Research and Innovation Agency, Yogyakarta, Indonesia

## ARTICLE INFO

## Keywords:

Streptomyces  
Secondary metabolite  
SARS-CoV-2  
AntiSMASH  
COVID-19

## ABSTRACT

COVID-19 is spreading rapidly yet there is no clinically proven drug available now. Soil-derived *Streptomyces* sp. GMR22 has a large genome size (11.4 Mbp) and a huge BGCs (Biosynthetic Gene Clusters) encoding secondary metabolites. This bacterium is a potential source for producing a wide variety of compounds which are able to block SARS-CoV-2, the causative agent of COVID-19. This study aimed to predict the secondary metabolites of *Streptomyces* sp. GMR22 and to evaluate the ability as SARS-CoV-2 inhibitor. The AntiSMASH 5.0 was used for genome mining analysis and targeted liquid chromatography-high resolution mass spectrometry (LC-HRMS) was used for metabolite analysis. In silico molecular docking was performed on important target proteins of SARS-CoV-2 i.e., spike protein (PDB ID: 6LXT), Receptor Binding Domain (RBD)-ACE2 (Angiotensin-Converting Enzyme 2) (PDB ID: 6VW1), 3CLpro (3-chymotrypsin-like protease) (PDB ID: 6M2N), and RdRp (RNA-dependent RNA polymerase) (PDB ID: 6M71). Two compounds from GMR22 extract, echoside A and echoside B were confirmed by targeted LC-HRMS and potential as SARS-CoV-2 inhibitor. Echoside A and echoside B showed higher docking score than remdesivir as COVID-19 drug on four target proteins, i.e., spike protein (−7.9 kcal/mol and −7.8 kcal/mol), RBD-ACE2 (−7.5 kcal/mol and −8.2 kcal/mol), 3CLpro (−8.4 kcal/mol and −9.4 kcal/mol) and RdRp (−7.3 kcal/mol and −8.0 kcal/mol). A combination of genome mining and metabolomic approaches can be used as integrated strategy to elucidate the potential of GMR22 as a resource in the discovery of anti-COVID-19 compound.

## 1. Introduction

*Streptomyces* is the most robust source for producing new bioactive compounds, antibiotics, and extracellular enzymes [1]. Previously identified *Streptomyces* from rhizosphere soil, Wanagama Forest, Gunungkidul, Yogyakarta, Indonesia, *Streptomyces* sp. GMR22 has 63 Biosynthetic Gene Clusters (BGCs), dominated by polyketide synthase (PKS) using AntiSMASH 3.0. Polyketide synthase involves in the production of polyketide compounds. Polyketide is a huge family of natural product class in which some clinically proven drugs, such as tetracycline, daunorubicin, erythromycin, rapamycin and lovastatin are included. Other than polyketide gene cluster, NRPS (Nonribosomal Peptide Synthetase), siderophore, RiPPs (Ribosomally Synthesized and

Post-Translationally Modified Peptides) and terpene were also found [2]. NRPS is enzyme which synthesize non-ribosomal peptides [3]. Siderophore encodes iron-chelating compounds, such as Desferrioxamine B, which have been predicted 100% could be produced by GMR22. Desferrioxamine B possessed anti-cancer activity in the cells of colon cancer [4]. GMR22 also predicted to harbour RiPPs gene, enabled this strain to generate class of cyclic or linear peptidic natural products [5]. Triterpenes are class of natural products composed of three terpene units. Previous study revealed that triterpenes had antiplasmodial activity [6]. Moreover, among genus *Streptomyces*, strain GMR22 has the highest number of BGCs, indicating that it is a prominent source for producing a wide variety of compounds [7, 8].

\* Corresponding author.

E-mail address: [jwidada@ugm.ac.id](mailto:jwidada@ugm.ac.id) (J. Widada).

**Table 1.** SARS-CoV-2 target proteins.

Target Protein	Protein ID	Activity
Spike glycoprotein	6LXT	Viral protein
RBD-ACE2	6VW1	Cell invasion
3CL Protease	6M2N	Viral Protein
RNA-dependent RNA polymerase	6M71	Viral Protein

**Table 2.** Biosynthetic gene clusters (BGCs) and secondary metabolites of *Streptomyces* sp. GMR22 based on the analysis of genome mining with AntiSMASH 5.0.

Cluster	Type	Size (bp)	Most similar known cluster (%)	
Cluster 1	T1PKS	40,540	Ansamitocin (19)	t1pks
Cluster 2	NRPS	53,306	Actinomycin (7)	NRPS
Cluster 3	T1PKS	5,152	Micromonolactam (100)	t1pks
Cluster 4	T1PKS	26,122	Hygrocin (74)	t1pks
Cluster 5	lanthipeptide	23,293	Reveromycin (9)	t1pks
Cluster 6	T1PKS, hglE-KS, bacteriocin	132,456	Bafilomycin (50)	t1pks
Cluster 7	T1PKS, NRPS-like	47,644	Ansatrienin (mycotrienin) (7)	nrps-t1pks
Cluster 8	T2PKS	72,503	Hexaricin (33)	t2pks
Cluster 9	terpene	21,100	Pristinol (100)	terpene
Cluster 10	NRPS, lanthipeptide	88,563	Lysolipin (4)	t2pks
Cluster 11	T1PKS, NRPS-like	44,220	Kedarcidin (1)	t1pks+t1pks
Cluster 12	Lasso peptide	22,385		
Cluster 13	siderophore	13,367	Natamycin (9)	t1pks
Cluster 14	butyrolactone	10,989	Salinipostin (22)	other
Cluster 15	NRPS	88,212	Glycinocin A (53)	NRPS
Cluster 16	T1PKS	7,155	Dihydrochalcomycin (19)	t1pks
Cluster 17	T1PKS	12,099	Hygrocin (16)	t1pks
Cluster 18	terpene	18,679	Hopene (53)	terpene
Cluster 19	ectoine	10,404	Ectoine (100)	Other
Cluster 20	T1PKS	9,683	Micromonolactam (100)	t1pks
Cluster 21	T1PKS	79,793	Elaiophylin (87)	t1pks
Cluster 22	hserlactone	20,755	Daptomycin (4)	NRPS
Cluster 23	butyrolactone	10,935	Meilingmycin (2)	t1pks
Cluster 24	NRPS, T3PKS, other	100,063	Feglymycin (78)	NRPS
Cluster 25	NRPS	39,173		
Cluster 26	NRPS	2,917		
Cluster 27	T1PKS	33,976	Geldanamycin (69)	t1pks
Cluster 28	T2PKS	72,491	Medermycin (50)	t2pks
Cluster 29	T1PKS	63,579	Mediomycin A (46)	polyketide
Cluster 30	Lasso peptide	22,645	Polyoxypeptin (5)	nrps-t1pks
Cluster 31	terpene	21,073	BE-43547 A1-C2 (15)	nrps-t1pks
Cluster 32	siderophore	13,770		
Cluster 33	terpene	22,390	Geosmin (100)	terpene
Cluster 34	T1PKS	114,376	Mediomycin A (50)	polyketide
Cluster 35	Aryl polyene, ladderane	42,383	WS9326 (25)	NRPS
Cluster 36	NRPS	44,010	Ochronotic pigment (75)	other
Cluster 37	siderophore	12,057		
Cluster 38	bacteriocin	11,340		

**Table 2 (continued)**

Cluster	Type	Size (bp)	Most similar known cluster (%)	
Cluster 39	T1PKS	62,547	S56-p1 (11)	NRPS
Cluster 40	siderophore	11,787	Desferrioxamine B (100)	other
Cluster 41	fused, T3PKS, NRPS	57,879	Pheganomycin (38)	nrps-ripp
Cluster 42	NRPS-like	25,322	Echosides (58)	NRPS
Cluster 43	ladderane, aryl polyene, NRPS	104,182	Skylamycin (46)	NRPS
Cluster 44	NRPS	34,118	Meridamycin (18)	nrps-t1pks
Cluster 45	indole	21,142	Terfestatin (61)	other
Cluster 46	NRPS	78,698	Leinamycin (5)	nrps-t1pks+transatpks
Cluster 47	terpene	22,129	Phenalinolactone (8)	terpene-saccharide
Cluster 48	terpene	20,908		
Cluster 49	NRPS-like	42,738	Echosides (11)	NRPS
Cluster 50	Beta-lactone	28,726	Sch47554/Sch47555 (7)	t2pks
Cluster 51	lanthipeptide	24,153		
Cluster 52	CDPS	20,650	Bicyclomycin (100)	other
Cluster 53	T1PKS	44,651	Mediomycin A (25)	polyketide
Cluster 54	T1PKS	59,316	Elaiophylin (45)	t1pks
Cluster 55	T1PKS	77,674	Nigericin (94)	t1pks
Cluster 56	T1PKS	126,000	Azalomycin F (82)	t1pks
Cluster 57	T3PKS, terpene, NRPS	40,798	Totopensamide (30)	nrps-t1pks
Cluster 58	T2PKS	72,515	Spore pigment (83)	t2pks
Cluster 59	terpene	21,190	2-methylisborneol (100)	terpene
Cluster 60	PKS-like	41,028	Galbonolides (20)	t1pks
Cluster 61	NRPS-like	44,028	Niphimycins C-E (6)	polyketide
Cluster 62	T1PKS	71,413	Meridamycin (55)	nrps-t1pks
Cluster 63	T1PKS, NRPS-like	45,285	Hygrocin (38)	t1pks
Cluster 64	T1PKS	61,962	Concanamycin A (17)	t1pks
Cluster 65	T1PKS	46,362	Salinomycin (8)	t1pks

T1PKS = Type I Polyketide Synthase; T2PKS = Type II Polyketide Synthase; T3PKS = Type III Polyketide Synthase; NRPS = Nonribosomal Polyketide Synthase; CDPS = Cyclodipeptide Synthase.

Global public health is still facing crisis due to the new virus, SARS-CoV-2 (Severe Acute Respiratory Syndrome Coronavirus-2), which originally emerged in Wuhan, China in December, 2019. This virus was declared as pandemic as of March, 11 2020 by the WHO (World Health Organization) and currently named as COVID-19 (Coronavirus disease) [9]. This virus is spreading rapidly yet there is no clinically effective drug available now which specifically treats COVID-19. It has been suggested that SARS-CoV-2 relied on viral spike protein and ACE2 receptor in the human body which found in the heart, lung, vessels, gut, kidney, testis and the brain for cell entry [10]. As for RNA viruses, RdRp is important for RNA synthesis. While, 3CLPro mediates maturation of non-structural proteins that essential during virus replication [11]. Therefore, we used RdRp (PDB ID: 6M71), and 3CLpro (PDB ID: 6M2N) as targets to inhibit the viral replication, while spike protein (PDB ID: 6LXT) and RBD-ACE2 (PDB ID: 6VW1) as targets to block the entry of SARS-CoV-2 [12], [13]. The compound found in this study could answer the urgent demand to counter SARS-CoV-2 (Severe Acute Respiratory Syndrome Corona Virus 2).

Complementary approaches, namely metabologenomics, was employed in the present study to find the targeted compounds which were directly correlated with GMR22 [14]. The genome mining approach predicted the secondary metabolites from GMR22 using a website-based bioinformatics platform. This research was combined with the metabolomic approach using mass spectrometry, LC-HRMS (Liquid Chromatography-High Resolution Mass Spectrometry), for thoroughly profiling targeted secondary metabolites synthesized by GMR22. Aiming to obtain secondary metabolites as SARS-CoV-2 inhibitors from *Streptomyces* sp. GMR22, this study gained insight of the secondary metabolites profile of GMR22, then subjected to in silico molecular docking against COVID-19 target proteins.

## 2. Material and methods

### 2.1. Microorganism strain

The *Streptomyces* sp. GMR22 isolated from the Cajuput rhizospheric soil of Wanagama forest, Indonesia was used in this study [8]. Strain GMR22 was maintained in International *Streptomyces* Project-2 (ISP-2) agar medium (Difco, Sparks, USA).

### 2.2. Genome mining analysis

A previous study had done genome sequencing for GMR22 [7]. This Whole Genome Shotgun project had been deposited at DDBJ/ENA/GenBank under accession JACGSQ000000000. The version described in this paper was version JACGSQ010000000. The genome of GMR2 was uploaded onto AntiSMASH 5.0 website (<https://antismash.secondarymetabolite.org>) to obtain gene cluster data [15].

### 2.3. Metabolomic profiling of extract

Strain GMR22 was grown on ISP-2 (International *Streptomyces* Project 2) agar for 7 days at 28 °C. The agar was cut into pieces (2 × 2 cm) and was put into 50 mL Tryptic Soy Broth (TSB) and incubated for 3 days in an incubator shaker at 28 °C. Five percent of inoculum was cultured in 1 L Erlenmeyer flask containing 20 g soluble starch; 0.5 g NaCl; 1 g KNO<sub>3</sub>; 0.5 g K<sub>2</sub>HPO<sub>4</sub>·3H<sub>2</sub>O; 0.5 g MgSO<sub>4</sub>·7H<sub>2</sub>O; 0.01 g FeSO<sub>4</sub>·7H<sub>2</sub>O for 8 days at 150 rpm on an incubator shaker at 28 °C. The cell and supernatant were separated for 10 min at 5000 rpm. The cell was extracted with methanol in low stirring for 30 min, then separated for 15 min at 4500 rpm. The

supernatant was taken as methanol crude extract and was evaporated to yield a gum.

The methanol crude extract was run on The Ultimate 3000 RSLCnano UHPLC-Q Exactive Orbitrap HRMS with an injection volume of 5 µL (concentration 10 µg/mL), a flow rate of 6.5 µL/min, and a column temperature of 30 °C. The Thermo Scientific™ Hypersil GOLD™ aQ analytical column was used for separation (50 mm length, 1.0 mm internal diameter, 1.9 µm particle size). Mobile phase A was 0.1% formic acid in MS grade water and mobile phase B was 0.1% formic acid in MS grade acetonitrile. The gradient program started at 5–50% for 13 min and the total run time was 30 min. The ESI ion source was set as follows: spray voltage of 3.80 kV, capillary temperature of 300 °C, and S-lens RF level of 50%. The compounds were detected in positive mode, Full Scan MS resolution of 70,000, targeted mode. The targeted mode used compounds information from the genome mining data. The compound information was obtained as mol file from PubChem or ChemSpider. The compounds were identified by Compound Discoverer 3.1 software. The peak extraction was done automatically by the software. The confirmation of each targeted compounds with respect to their parent compounds was achieved by considering isotope pattern match. Isotope pattern match in LC-HRMS could identify various relative abundance of isotope in the targeted compounds. Additionally, composition change was taken into account. All compound IDs were matched within +/- 5 ppm mass tolerance.

### 2.4. In silico molecular docking

Molecular docking was used to predict the binding affinity between the GMR22 targeted new compound against the target proteins of COVID-19. The target proteins used in this study were downloaded from Protein Data Bank, i.e., spike protein (PDB ID: 6LXT), RBD-ACE2 (PDB ID: 6VW1), 3CLpro (PDB ID: 6M2N), and RdRp (PDB ID: 6M71). The target protein list is given in Table 1. The 2D conformers of the GMR22 targeted compound were obtained from ChemSpider, then converted into 3D conformer using MarvinSketch tools (<https://chemaxon.com>). All water, ions, and other small molecules were removed from the target proteins, and then the hydrogen atoms were added using auto dock tools. The molecular docking was carried out by using Autodock Vina [16]. The docking result was binding affinity (kcal/mol) with a root mean square deviation (RMSD) score of less than 2 Å. Meanwhile, DisCoVery studio visualizer (DS visualizer) tool was used for visualizing the binding interaction of the GMR22 targeted compound on the

**Table 3.** Metabolomic analysis of *Streptomyces* sp. GMR22 extract using targeted LC-HRMS based on predicted compound from genome mining analysis.

Parent Compound	Formula	Molecular Weight	Composition Change	RT [min]	Area (Max.)
Natamycin	C <sub>6</sub> H <sub>11</sub> NO <sub>4</sub>	161.06881	-(C <sub>27</sub> H <sub>36</sub> O <sub>9</sub> )	4.606	321808049.5
Elaiophylin	C <sub>6</sub> H <sub>12</sub> O <sub>4</sub>	148.07356	-(C <sub>48</sub> H <sub>76</sub> O <sub>14</sub> )	7.037	3873193.757
Hygrocin A	C <sub>7</sub> H <sub>8</sub> O <sub>2</sub>	124.05243	-(C <sub>21</sub> H <sub>23</sub> NO <sub>6</sub> )	7.148	158292572.2
Echside A	C <sub>25</sub> H <sub>24</sub> O <sub>9</sub>	468.14203	No	7.368	29448524.78
Echside B	C <sub>25</sub> H <sub>24</sub> O <sub>9</sub>	468.14203	No	7.368	29448524.78
Echside C	C <sub>18</sub> H <sub>14</sub> O <sub>3</sub>	278.09429	-(C <sub>6</sub> H <sub>8</sub> O <sub>6</sub> )	8.975	55169603.62
Desferrioxamine B	C <sub>11</sub> H <sub>20</sub> N <sub>2</sub> O <sub>5</sub>	260.13722	-(C <sub>14</sub> H <sub>28</sub> N <sub>4</sub> O <sub>3</sub> )	13.422	3710903011
Kedarcidin	C <sub>8</sub> H <sub>15</sub> NO <sub>3</sub>	173.10519	-(C <sub>45</sub> H <sub>45</sub> C <sub>1</sub> N <sub>2</sub> O <sub>13</sub> )	14.324	122233428.1
Geldamycin	C <sub>13</sub> H <sub>18</sub> O <sub>5</sub>	254.11542	-(C <sub>17</sub> H <sub>24</sub> N <sub>2</sub> O <sub>3</sub> )	19.514	25962945.37
Bafilomycin B1	C <sub>35</sub> H <sub>56</sub> O <sub>9</sub>	620.39243	-(C <sub>9</sub> H <sub>9</sub> NO <sub>4</sub> )	25.472	6677673.906
Medermycin	C <sub>22</sub> H <sub>20</sub> O <sub>9</sub>	428.11073	-(C <sub>2</sub> H <sub>7</sub> N) + (O)	26.035	1251745.932
Daptomycin	C <sub>10</sub> H <sub>21</sub> NO	171.16231	-(C <sub>62</sub> H <sub>80</sub> N <sub>16</sub> O <sub>25</sub> )	26.352	15124300.16
Skyllamycin A	C <sub>12</sub> H <sub>13</sub> NO	187.09971	-(C <sub>63</sub> H <sub>81</sub> N <sub>11</sub> O <sub>19</sub> )	26.482	19901446.49
Glycinocin A	C <sub>15</sub> H <sub>28</sub> O <sub>2</sub>	240.20893	-(C <sub>42</sub> H <sub>62</sub> N <sub>12</sub> O <sub>17</sub> )	26.523	135669155.6

RT: retention times (minutes).

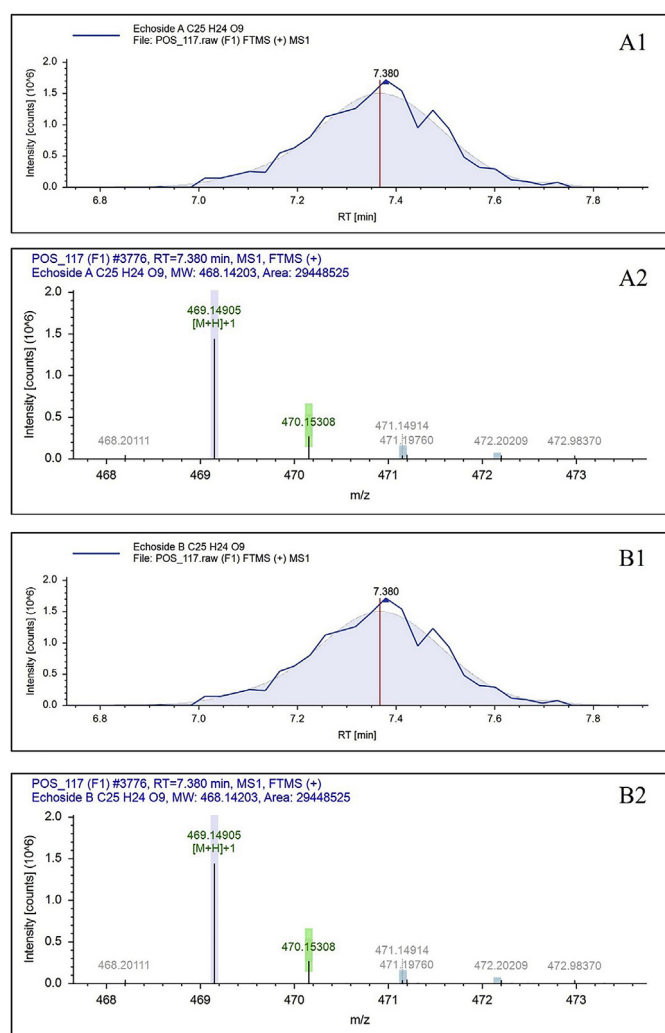


**Figure 1.** Echoside A (A) and Echoside B (B). Chromatogram (1) and mass spectra (2) of *Streptomyces* sp. GMR22 extract detected on LC-HRMS analysis.

binding site of proteins [17]. The molecular docking was performed in the Windows 10 Operating system, AMD A8 7410 (Quad-core; 2,2 GHz), with 4 GB RAM.

### 3. Results and discussion

#### 3.1. Genome mining analysis

Genome mining tool, AntiSMASH 5.0. is a well-known online platform to predict secondary metabolites synthesized by bacteria and various gene clusters involved in the secondary metabolite biosynthesis, such as polyketide synthase, nonribosomal synthetase, terpene, and RiPPs (ribosomally synthesized and post-translationally modified peptides) [15]. AntiSMASH is linked automatically to MIBiG (Minimum Information about Biosynthetic Gene Cluster) 2.0, representing the percent of similarity to known products and its related references. Compared to the bioinformatics analysis from the previous study, this study had more actual data due to the periodic database update of AntiSMASH. The database update was based on the latest researches about secondary metabolites from bacteria. The genome mining result is shown in Table 2.

Table 2 shows 65 biosynthetic gene clusters (BGCs) of *Streptomyces* sp. GMR22, involved in the secondary metabolism. The total number of BGCs is the highest among other *Streptomyces* [7] as the average number of BGCs in *Streptomyces* was 30 gene clusters [18]. More than a third of BGCs were dominated by polyketide synthase, consisting of pure 18 Type I polyketide synthase (T1PKS), 3 Type II polyketide synthase (T2PKS), 3 hybrid Type I polyketide synthase, and 3 hybrid Type III polyketide synthase. In addition to PKS gene cluster, pure NRPS, NRPS hybrid, siderophore, and terpene gene cluster were found as well. However, the number was much less than that of PKS gene cluster. Polyketide synthase (PKS) is well-recognized for producing diverse compounds with various bioactivity [4], for example, desferrioxamine B and elaiophylin. Both have been reported as anticancer [19, 20]. Six gene clusters had 100% similarity to known BGC products, namely pristinol (terpene), ectoine (ectoine), geosmin (terpene), desferrioxamine B (siderophore), bicyclo-mycin (cyclodipeptide synthase), 2-methylisoborneol (terpene), while others had mostly under 100% similarity to previously identified compounds. This genome mining result was able to predict the large variety of metabolites from GMR22.

**Table 4.** Binding energy of the GMR22 targeted compounds and reference compound against the target proteins of SARS-CoV-2.

Compounds	Binding energy (kcal/mol)			
	6LXT (spike protein)	6VW1 (RBD-ACE2)	6M2N (3CLpro)	6M71 (RdRp)
Remdesivir*	-6.9	-6.7	-6.5	-6.4
Natamycin	-9.3	-9.6	-9.9	-8.8
Elaiophylin	-10.2	-10.9	-10.9	-9.9
Hygrocin A	-9.2	-9.4	-9.7	-8.9
Echoside B	-7.8	-8.2	-9.4	-8.0
Echoside A	-7.9	-7.5	-8.4	-7.3
Echoside C	-8.1	-7.7	-8.6	-8.1
Desferrioxamine B	-4.9	-5.6	-6.2	-4.8
Kedarcidin	-10.0	-10.7	-9.4	-10.0
Geldanamycin	-6.6	-7.4	-7.0	-7.1
Bafilomycin B1	-8.8	-9.8	-9.6	-8.9
Medermycin	-9.4	-8.6	-9.1	-7.8
Daptomycin	-8.9	-9.1	-9.3	-8.9
Skyllamycin A	-8.4	-10.7	-8.1	-7.1
Glycinocin A	-7.8	-9.0	-7.4	-7.8

\* Reference drug.

### 3.2. Targeted metabolomic analysis

AntiSMASH 5.0 was used as a guide for the secondary metabolites profiling of GMR22 which was further confirmed by targeted metabolomic analysis with LC-HRMS. The compounds were detected by LC-HRMS showed in Table 3. The full spectra of targeted LC-HRMS showed in Supplementary Figure S1 and expected compounds data of targeted LC-HRMS showed in Supplementary Table S1. Most of the compounds detected by LC-HRMS underwent composition change of the target parent compound based on the genome mining analysis. The compounds predicted by using antiSMASH have similarity of 1–100% with BGCs from the database. This means that the compounds produced by GMR22 are not exactly the same as the compounds predicted by genome mining. Meanwhile, echoside A and echoside B were compounds which had been predicted in the genome mining analysis and had been detected in LC-HRMS. These compounds have  $C_{25}H_{24}O_9$  formula and

468.14203 of molecular weight (Da). The echoside A and echoside B spectrum and ionization showed in Figure 1. These compounds were detected at 7.3 min of RT and there was no composition change from parent compound as a target. These results confirmed that echoside A and echoside B were produced by *Streptomyces* sp. GMR22 based on both on genomic analysis using AntiSMASH and metabolomic analysis using LC-HRMS. Both appeared same, but the only different were their orientation. They are isomers.

### 3.3. In silico molecular docking

The number of target proteins that hold a pivotal role in viral entry and replication become attractive SARS-CoV-2 drug targets. Targeting RdRp, and 3CLpro was considered efficient to inhibit the enzyme function during SARS-CoV-2 intracellular replication, while targeting RBD-ACE2 and spike glycoprotein was efficient to prevent SARS-CoV-2 from

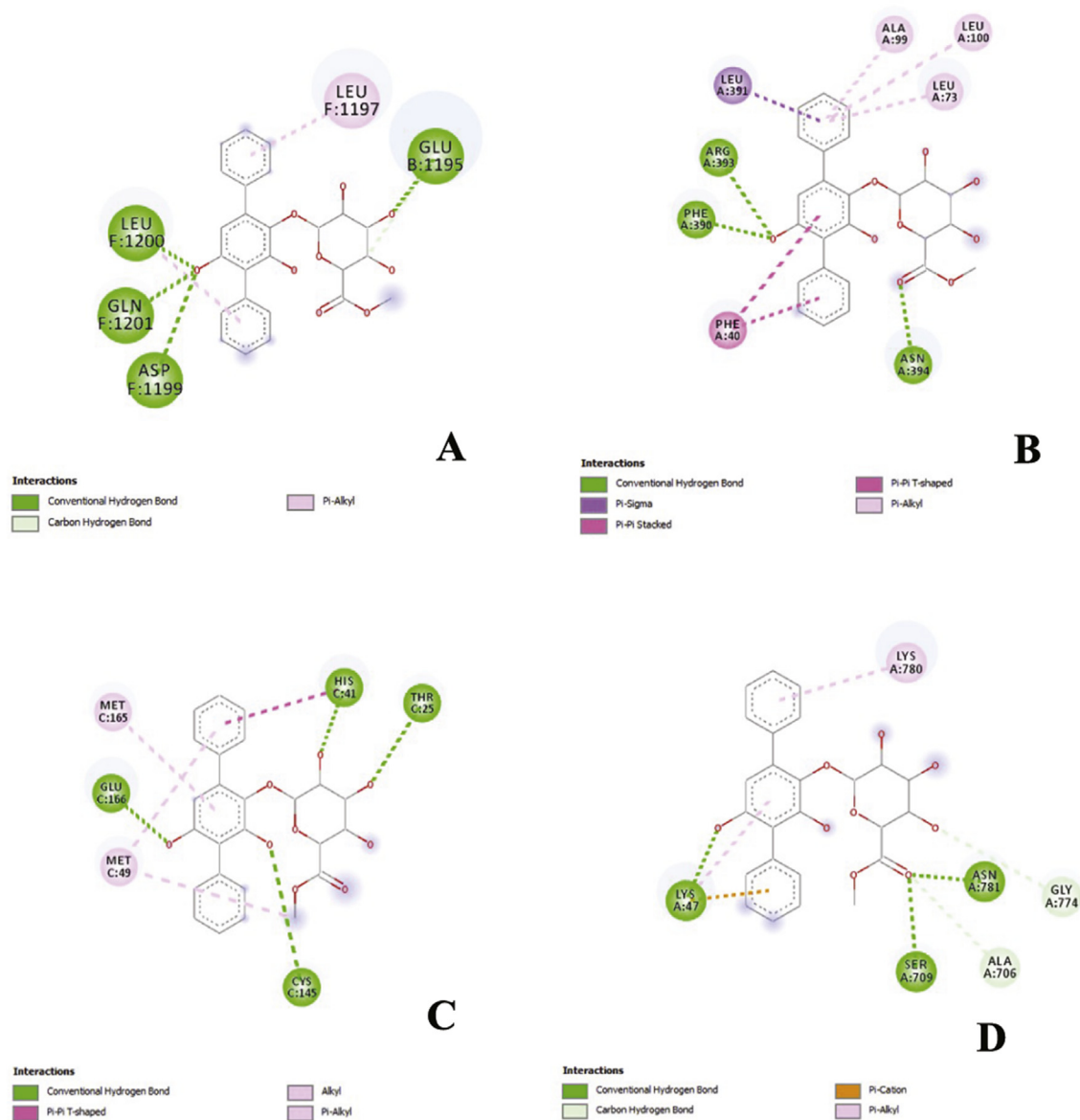
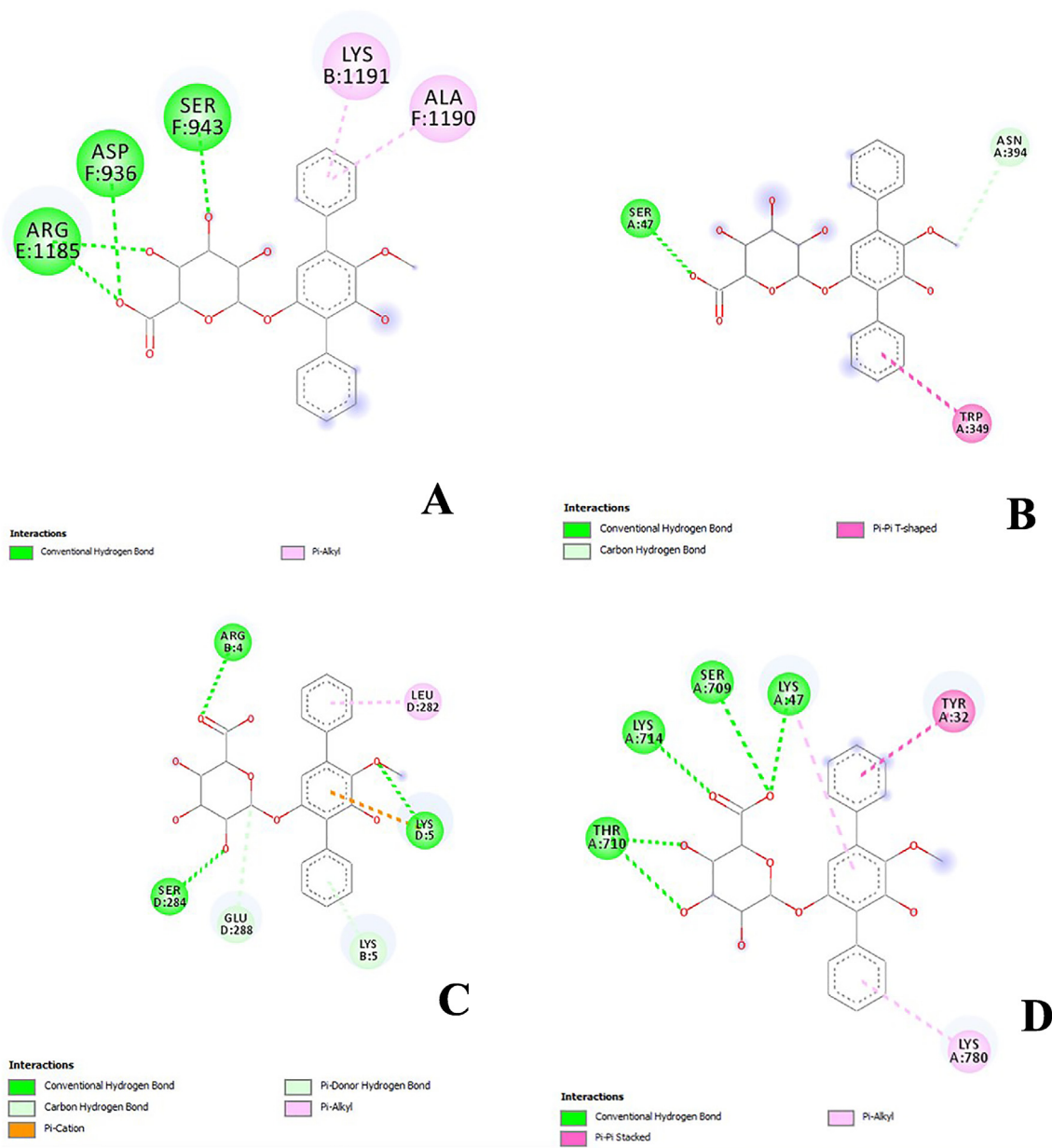


Figure 2. Binding visualization of echoside A with spike protein (A), RBD-ACE2 (B), 3CLpro (C), and RdRp (D), respective interacting amino acid residues.





**Figure 4.** 2D visualization of binding between echoside B with spike protein (A), RBD-ACE2 (B), 3CLpro (C), and RdRp (D), respective interacting amino acid residues.

MET (165) and MET (25) in pi-alkyl bond with the target site (3CLPro) (Figure 2C). In RdRp protein, Echoside A formed with LYS (47), SER (709), and ASN (781) in hydrogen bond, ALA (706) and GLY (774) in carbon hydrogen bond, while LYS (780) showed pi-alkyl bond with protein target site (Figure 2D). The 3D conformation of echoside A and target proteins showed the amino acid interaction in 3D protein conformation with solvent accessible surface (SAS) for this binding site is computed. SAS is often used when calculating the transfer free energy required to move a biomolecule from aqueous solvent to a non-polar solvent such as a lipid environment. The SAS value of the echoside A with the target proteins scored between 10.0 – 22.5 (Figure 3). Echoside B formed interaction with the following residues of spike protein, LYS (1191) and ALA (1190) showed interaction with echoside B in pi-alkyl

bond, ASP (936), SER (943), and ARG (1185) interact with hydrogen bond (Figure 4A). In RBD-ACE2 protein, Echoside B formed with SER (47) in hydrogen bond, ASN (394) in carbon hydrogen bond, TRP (349) in pi-pi T-shaped bond (Figure 4B). Echoside B formed with ARG (4), SER (284), LYS (5) in hydrogen bond, LYS (5) and GLU (288) in carbon hydrogen bond, and LEU (282) in pi-alkyl bond with the target site (3CLPro) (Figure 4C). In RdRp protein, Echoside B formed with LYS (47), SER (709), LYS (714), and THR (710) in hydrogen bond, TYR (32) in pi-pi stacked bond, while LYS (780) showed pi-alkyl bond with protein target site (Figure 4D). The amino acid interaction of echoside B with the targets protein in 3D protein conformation is displayed in Figure 5. The SAS value of the echoside B with the targets protein scored between 10.0 – 22.5.

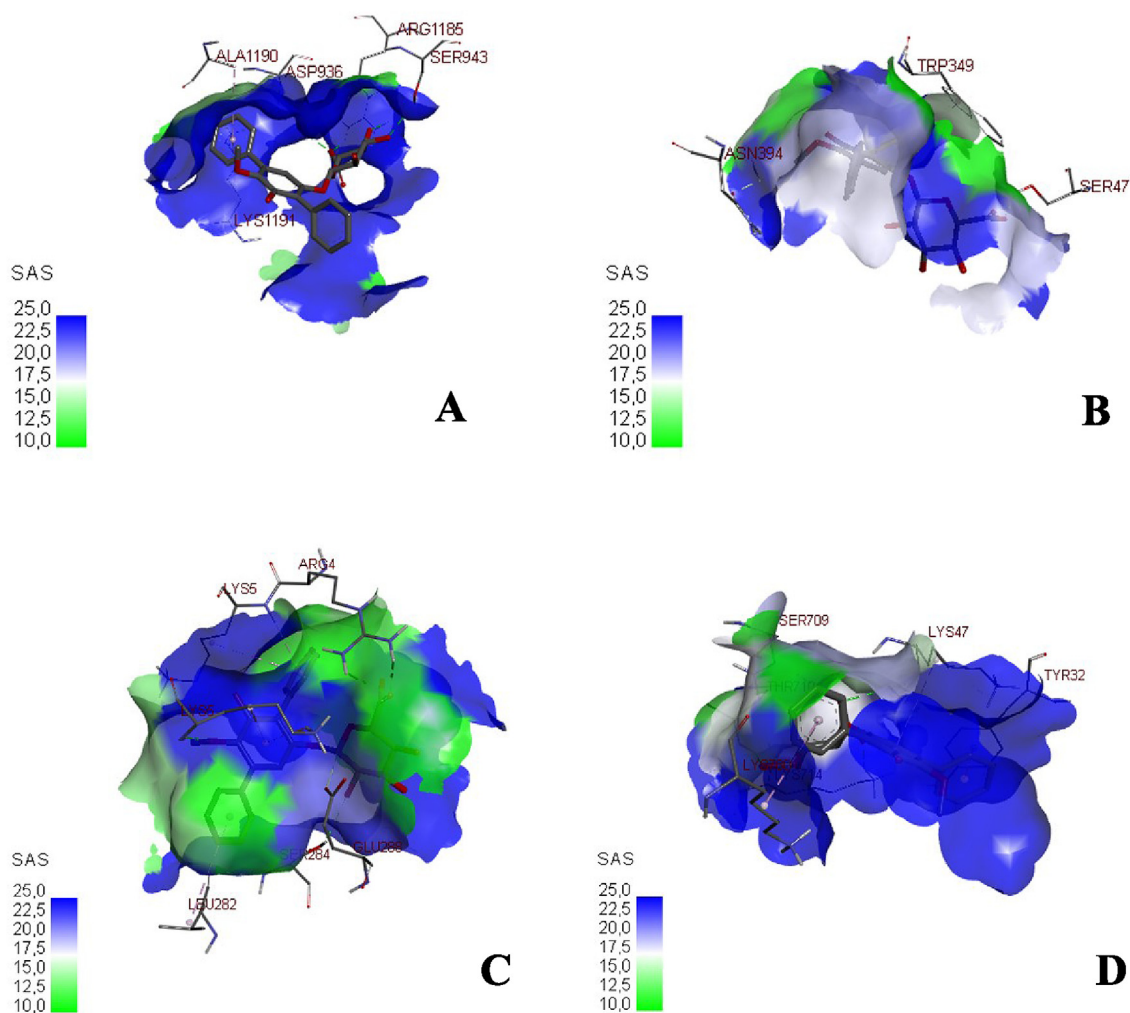


**Figure 5.** 3D visualization of binding between echoside B with spike protein (A), RBD-ACE2 (B), 3CLpro (C), and RdRp (D), respective interacting amino acid residues.

#### 4. Conclusions

The present study was carried to explore novel inhibitors of SARS-CoV-2 directly correlated with soil-derived bacterium, *Streptomyces* sp. GMR22, by applying both genome mining and metabolomic approaches. Echoside A and Echoside B showed the best binding interaction with three target proteins, i.e., spike protein, RBD-ACE2, and 3CLpro. Furthermore, echoside A and echoside B displayed better docking score than remdesivir, showed high potential as antiviral, and have been tested as antiviral in other previous study, thus echoside A and echoside B could be utilized for further exploration as an antiviral agent for SARS-CoV-2.

#### Declarations

##### Author contribution statement

Yohana Nadia Melinda: Conceived and designed the experiments; Performed the experiments; Analyzed and interpreted the data; Wrote the paper.

Jaka Widada: Conceived and designed the experiments; Analyzed and interpreted the data; Contributed reagents, materials, analysis tools or data.

Tutik Dwi Wahyuningsih: Conceived and designed the experiments; Analyzed and interpreted the data; Contributed reagents, materials, analysis tools or data.

Rifki Febriansah: Performed the experiments; Analyzed and interpreted the data; Wrote the paper.

Emad Damayanti: Conceived and designed the experiments; Performed the experiments; Analyzed and interpreted the data; Contributed reagents, materials, analysis tools or data; Wrote the paper.

Mustofa Mustofa: Conceived and designed the experiments; Analyzed and interpreted the data; Contributed reagents, materials, analysis tools or data.

##### Funding statement

This work was supported by Indonesian Ministry of Research, Technology and Higher Education (3402/UNI.DITLIT/DIT-LIT/PT/2020).

##### Data availability statement

Data associated with this study has been deposited at GenBank under the accession number JACGSQ01000000.

##### Declaration of interests statement

The authors declare no conflict of interest.

### Additional information

Supplementary content related to this article has been published online at <https://doi.org/10.1016/j.heliyon.2021.e08308>.

### Acknowledgements

The authors thank Tri Purwanti and Hendy Dwi Warmiko for the technical support.

### References

- [1] O.S. Olanrewaju, O.O. Babalola, Streptomycetes: implications and interactions in plant growth promotion, *Appl. Microbiol. Biotechnol.* 103 (3) (2019) 1179–1188.
- [2] C. Herdini, et al., Secondary bioactive metabolite gene clusters identification of anticandida-producing streptomycetes Sp. GMR22 isolated from Wanagama forest as revealed by Genome mining approach, *Indones. J. Pharm.* 28 (1) (2017) 26–33.
- [3] H. Wang, D.P. Fewer, L. Holm, L. Rouhiainen, K. Sivonen, Atlas of nonribosomal peptide and polyketide biosynthetic pathways reveals common occurrence of nonmodular enzymes, *Proc. Natl. Acad. Sci. U. S. A.* 111 (25) (2014) 9259–9264.
- [4] O. Salis, A. Bedir, V. Kilinc, H. Alacam, S. Gulden, A. Okuyucu, The anticancer effects of desferrioxamine on human breast adenocarcinoma and hepatocellular carcinoma cells, *Cancer Biomarkers* 14 (6) (2014) 419–426.
- [5] Z. Zhong, B. He, J. Li, Y.X. Li, Challenges and advances in genome mining of ribosomally synthesized and post-translationally modified peptides (RiPPs), *Synth. Syst. Biotechnol.* 5 (3) (2020) 155–172.
- [6] M. Isaka, A. Yangchum, P. Rachtawee, S. Komwijit, A. Lutthisungneon, Hopane-type triterpenes and binaphthopyrones from the scale insect pathogenic fungus *aschersonia paraphysata* BCC 11964, *J. Nat. Prod.* 73 (4) (2010) 688–692.
- [7] C. Herdini, et al., Diversity of nonribosomal peptide synthetase genes in the Anticancer Producing actinomycetes isolated from marine sediment in Indonesia, *Indones. J. Biotechnol.* 20 (1) (2016) 34.
- [8] R. Nurjasmı, J. Widada, N. Ngadiman, Diversity of actinomycetes at several forest types in Wanagama I Yogyakarta and their potency as a producer of antifungal compound, *Indones. J. Biotechnol.* 14 (2) (2009) 1196–1205.
- [9] E.A. Bhat, et al., SARS-CoV-2: insight in genome structure, pathogenesis and viral receptor binding analysis – an updated review, *Int. Immunopharm.* 95 (2021) 107493.
- [10] X. Xu, et al., Evolution of the novel coronavirus from the ongoing Wuhan outbreak and modeling of its spike protein for risk of human transmission, *Sci. China Life Sci.* 63 (2020) 457–460.
- [11] S. Joshi, M. Joshi, M.S. Degani, Tackling SARS-CoV-2: proposed targets and repurposed drugs, *Future Med. Chem.* 12 (7) (2020) 1579–1601.
- [12] D.C. Hall, H.F. Ji, A search for medications to treat COVID-19 via in silico molecular docking models of the SARS-CoV-2 spike glycoprotein and 3CL protease, *Trav. Med. Infect. Dis.* 35 (2020) 101646.
- [13] J. Shang, et al., Structural basis of receptor recognition by SARS-CoV-2, *Nature* 581 (2020) 221–224.
- [14] J.T. Gosse, S. Ghosh, A. Sproule, D. Overy, N. Cheeptham, C.N. Boddy, Whole genome sequencing and metabolomic study of cave Streptomycetes isolates ICC1 and ICC4, *Front. Microbiol.* 10 (2019) 1–12.
- [15] K. Blin, et al., AntiSMASH 5.0: updates to the secondary metabolite genome mining pipeline, *Nucleic Acids Res.* 47 (2019) W81–W87.
- [16] A.J. Trott, O. Olson, "Autodock vina, Improving the speed and accuracy of docking, *J. Comput. Chem.* 31 (2) (2019) 455–461.
- [17] D. Studio, Dassault Systemes BIOVIA, Discovery Studio Modelling Environment, Release 4.5, Accelrys Softw. Inc., 2015.
- [18] N.M. Ishaque, et al., Isolation, genomic and metabolomic characterization of *Streptomyces tendae* VITAKN with quorum sensing inhibitory activity from Southern India, *Microorganisms* 8 (1) (2020).
- [19] X. Zhao, et al., Elaiophylin, a novel autophagy inhibitor, exerts antitumor activity as a single agent in ovarian cancer cells, *Autophagy* 11 (10) (2015) 1849–1863.
- [20] A.J. Van Heel, A. De Jong, C. Song, J.H. Viel, J. Kok, O.P. Kuipers, BAGEL4: a user-friendly web server to thoroughly mine RiPPs and bacteriocins, *Nucleic Acids Res.* 46 (2018) W278–W281.
- [21] M. Wang, et al., Remdesivir and chloroquine effectively inhibit the recently emerged novel coronavirus (2019-nCoV) in vitro, *Cell Res.* 30 (3) (2020) 269–271.
- [22] J. Zhu, et al., Identification and catalytic characterization of a nonribosomal peptide synthetase-like (NRPS-like) enzyme involved in the biosynthesis of echosides from *Streptomyces* sp. LZ35, *Gene* 54 (2) (2014) 352–358.
- [23] P. Luthra, et al., Topoisomerase II inhibitors induce DNA damage-dependent interferon responses circumventing ebola virus immune evasion, *mBio* 8 (2) (2017) e00368-17.